Article title

Integrated transcriptional analysis reveals gene expression-based AML subtypes with distinct outcomes and drug responses

Author names

Jeppe F Severens[1,2,3], E Onur Karakaslar[1,2,3], Bert A van der Reijden[4], Elena Sánchez-López[3,5], Redmar R van den Berg[6], Constantijn JM Halkes[7], Peter van Balen[7], Hendrik Veelken[3,7], Marcel JT Reinders[1,2,3], Marieke Griffioen[7], Erik B van den Akker[1,2,3]

Affiliations

[1]Department of Biomedical Data Sciences, Leiden University Medical Center, Leiden, The Netherlands

[2]Pattern Recognition & Bioinformatics, Delft University of Technology, Delft, The Netherlands

[3]Leiden Center for Computational Oncology, Leiden University Medical Center, Leiden, The Netherlands

[4]Laboratory of Hematology, Department of Laboratory Medicine, Radboud University Medical Center, Nijmegen, The Netherlands

[5]Center for Proteomics and Metabolomics, Leiden University Medical Center, Leiden, The Netherlands

[6]Department of Human Genetics, Leiden University Medical Center, Leiden, The Netherlands

[7]Department of Hematology, Leiden University Medical Center, Leiden, The Netherlands

Abstract

Subtyping of acute myeloid leukaemia (AML) has made significant progress, exemplified by the recent classification updates by the World Health Organization and International Consensus Classification. AML subclassification is predominantly genetics-based, despite research showing the benefits of transcriptomic profiling on top of known genetic markers. However, a comprehensive survey of subtypes in AML defined by gene expression has yet to be performed. To this end, we integrated mRNAseq data from 1337 patients and five studies, with corresponding biological and clinical data. We defined 19 gene expression-based subtypes, further stratifying AML. We found that KMT2A leukaemias with fusion partners MLLT3, MLLT10 and MLLT1 clustered together, while KMT2A-MLLT4 displayed a distinct gene expression pattern, suggesting differences in their aetiology. We discovered a transcriptional CEBPA subtype, of which only 40% had a CEBPA bZIP indel. Regardless of mutation status, all patients within this CEBPA cluster had the same favourable outcome. We found four NPM1-enriched transcriptomic subtypes, each with distinct co-mutation patterns and associated ex-vivo drug responses. Similarly, we identified nine AML with myelodysplasia-related changes (AML-MRC) subtypes, dividing a subtype making up one-third of the AML patients into novel groups with different outcomes and drug response profiles. In conclusion, we provide an unprecedented overview of the transcriptomic subtypes in AML and illustrate their potential for AML diagnostics.

Introduction

Acute myeloid leukaemia (AML) is a group of blood cancers caused by an aggressive proliferation of myeloid progenitor cells upon acquiring genetic abnormalities.[1,2] Systematic genomic studies have identified many recurrent genetic abnormalities (RGA) in AML, including chromosomal aberrations, indels, and point mutations.[3–7] Significant progress has been made in the classification of AML and based on these RGAs, the current World Health Organization (WHO 2022) and International Consensus Classification (ICC 2022) define several AML subtypes, as well as a heterogeneous subtype of AML with myelodysplasia-related changes (AML-MRC).[2,8] RGAs are essential for risk stratification and increasingly guide targeted treatment of specific aberrations with new drugs.[1,9]

AML subclassification is currently genetics-based, but a wealth of transcriptomic data is available with great potential to improve clinical AML subtyping.[3–5,10–15] Exploring the transcriptome has led to the discovery of the favourable CEBPA mutated AML subtype[16,17], allowing for improved AML risk stratification. Furthermore, gene expression profiling distinguishes at least two classes of NPM1-mutated AML with different drug responses[18,19], showing how transcriptomics can improve treatment selection. For AML-MRC, similar transcriptomic-based stratification would be beneficial because an adverse outcome characterises AML-MRC. At the same time, the current heterogeneity is problematic for individualised treatment.[20,21] While these studies underpin the potential of transcriptomic subtyping on top of known genetic markers, a comprehensive survey of subtypes defined by gene expression in AML is currently lacking.

Therefore, we integrated four publicly available and our in-house bulk mRNAseq datasets with corresponding mutation, fusion, and cytogenetics data. We annotated the samples according to the WHO 2022 and ICC 2022 guidelines to align with the latest clinical standards. By harmonising several studies, we increase statistical power and give an unprecedented overview of the transcriptomic landscape of AML. We define transcriptional AML subtypes with specific marker gene expression, mutation statuses and states of maturation arrest. We show that these novel subtypes are clinically relevant based on specific outcomes and ex-vivo responses to therapeutic agents.

Methods

Transcriptomic data

For this study, we acquired transcriptional data of AML patients from blood or bone marrow from the cohorts BEAT[5] (n = 450), TARGET[4] (n = 187), TCGA[3] (n = 151), and Leucegene[11–14] (n = 449), and our earlier published in-house LUMC[22] dataset (n = 100) (details in **Supplemental Methods**). The methods of whole messenger transcriptome sequencing are available in each of the referenced studies.

For BEAT, TARGET and TCGA the gene expression was already quantified, as described in their respective studies. To harmonise the analysis pipeline we quantified gene expression for the Leucegene and LUMC data in a similar manner. We performed quality control and alignment as earlier described[22] and quantified gene expression using HTSeq[23] with the GENCODE v22 annotations.[24]

We then batch-corrected the gene expression data with Combat-Seq[25] for the variables study, sex and source tissue to allow for a combined analysis. The success of the batch effect correction was quantified using the kBET measure.[26] The expression data was normalised using DESeq2 with the geometric mean and variance stabilising transformation.[27]

Genetic and patient data

We acquired corresponding genetic data for the transcriptomic samples in the form of mutation calling, fusion calling and cytogenetics data, patient characteristics on sex, age, blast percentage, French-American-British (FAB) classification, and survival data.

We harmonised the data by standardising gene symbols, FAB classification annotations, and we subclassified samples according to the WHO 2022[2] and ICC 2022[8] using genetic data. Samples for which we found no RGA – but that did have all mutation, fusion and karyotyping available – were annotated as “AML, other RGA” for the WHO and “AML, NOS” for the ICC. We subclassified samples with missing genetic data and no RGA found in the available data or no data as “Inconclusive”.

Clustering and differential gene expression analysis

For gene expression-based clustering, we generated a nearest neighbour graph using the 2000 most variable genes as per the median absolute deviation, on which clustering was performed using the

Leiden algorithm.[28] We performed the clustering as an iterative process till the clustering captured genetic AML classes in individual clusters as well as possible.

Differential gene expression analysis between the clusters was performed using DESeq2[27], using the uncorrected gene counts as input. We performed a one versus rest analysis to identify differentially expressed genes in one cluster compared to all others combined. We included the variables study, sex and source tissue in the analysis to correct for their effect.

Genetic aberration enrichment analysis

We performed an enrichment analysis to evaluate if aberrations occurred more in a cluster than in others. To filter, we removed aberrations that were only found in one study or that occurred in less than one per cent of the samples. We tested for enrichment per aberration by performing a Fisher-exact test for one cluster versus all others and adjusted p-values using the Benjamini-Hochberg procedure. We considered aberrations as enriched in a cluster if they had an adjusted p-value lower than 0.05 and occurred in at least 10% of the samples in a cluster.

Cell-type score

We created a cell type score to evaluate the differentiation arrest status of samples, using the mean expression of 30 marker genes for several haematological cells as reported by van Galen and colleagues.[29] We generated this score per cell type, per sample.

Drug response analysis

To analyse drug response differences between clusters, we used the ex-vivo drug response data of the BEAT[5] cohort. The drug response was reported as area under the curve (AUC) and was available for up to 122 small-molecule drugs for 330 samples. We tested for differences in drug response with a Wilcoxon test by comparing the AUC values of one cluster to the AUC values of all other clusters. The p-values were adjusted using the Benjamini-Hochberg procedure. We considered samples in a cluster sensitive to a drug if the median AUC was lower in that cluster compared to the median of the combined other clusters or resistant to a drug if the median AUC was higher in that cluster compared to the median of the combined other clusters and if the adjusted p-value was below 0.05.

Data Sharing Statement

Differential gene expression results are available from **Appendix 1**. Data supplements are available in the online version of this article. For further data requests please contact e.b.van_den_akker@lumc.nl.

Results

Transcriptomic analysis further stratifies AML

After harmonising our dataset of 1337 patients (**Figure 1A,B, Supplemental figures 1-3**), we identified 19 transcriptional clusters (**Figure 1C, Supplemental table 1**). Enrichment analysis found several significantly enriched RGAs in the clusters (**Figure 1D**, exact p-values in **Supplemental table 2**). We then used enriched aberrations and the distribution of WHO 2022 and ICC 2022 diagnoses (**Supplemental Figure 4**) to name our transcriptional subtypes (marked by ^{t}).

We found that the gene expression-based subtypes confirmed the genetic RUNX1-RUNX1T1, CBFB-MYH11, PML-RARA fusions and NUP98 rearrangements subtypes of the WHO 2022 and ICC 2022. The clustering split MECOM rearranged samples between six AML-MRC clusters, and we observed no specific pattern for the BCR-ABL1 and DEK-NUP214 fusion genes. These three fusions occur with a low frequency in AML, and the lack of a distinctive expression pattern might be attributed to limited statistical power.

Contrasting genetic subtyping, we found that based on gene expression, refinements in subtype definitions were possible for AML with KMT2A rearrangement and AML with CEBPA mutations. Also, we found four transcriptional subtypes of AML, NPM1-mutated patients, and nine transcriptional subtypes of AML-MRC patients, providing essential evidence for improvements in AML subtyping for these patient groups.

KMT2A fusions with MLLT3, MLLT10, and MLLT1 share a specific gene expression signature

The recent update of the WHO subclassification merged all KMT2A fusions into one AML subtype, while the ICC defines AML with a KMT2A-MLLT3 fusion and AML with other KMT2A rearrangements.[2,8] We found that the KMT2A^{t} cluster was enriched for KMT2A-MLLT3, KMT2A-MLLT10, and KMT2A-MLLT1, while KMT2A-MLLT4 grouped together and KMT2A-ELL samples were located in NPM1-erriched clusters (**Table S2, Figure 2A,B)**. KMT2A-MLLT3, KMT2A-MLLT10, and

KMT2A-MLLT1 had a similar expression pattern, while KMT2A-MLLT4 and KMT2A-ELL showed different expression patterns (**Figure 2D**).

Differential gene expression analysis (**Appendix 2**) showed that high expression of the homeobox family genes HMX2 and HMX3 (**Figure 2C**) characterised the KMT2A^t cluster. Both of these genes are known to induce myeloid differentiation arrest, suggesting a causal role in AML pathogenesis for the KMT2A^t cluster.[30] In addition, we found high expression of XAGE1A and XAGE1B, which studies have proposed as potential targets for immunotherapy.[31,32] Based on gene expression, we could not confirm established genetic groupings of KMT2A rearrangements, but rather find KMT2A-MLLT3, KMT2A-MLLT10, and KMT2A-MLLT1 together and KMT2A-MLLT4 separately to form two transcriptional groups, suggesting marked differences in the disease.

The CEBPA^t cluster gene expression signature indicates a favourable prognosis even in the absence of a CEBPA bZIP in-frame mutation

As acknowledged in the ELN2022 guidelines, patients with CEBPA bZIP inframe-mutation have the same favourable prognosis as patients with a biallelic CEBPA mutation.[1,33,34] Unexpectedly, only 40% of the samples within the CEBPA^t cluster carried a CEBPA bZIP in-frame mutation. The remaining samples either had different types of mutations in the bZIP area (7%), only an N-terminal mutation (23%), or no CEBPA mutation (30%), while exhibiting a similar expression profile (**Figure 3A**). Several samples with a single bZIP or N-terminal mutation were located outside the CEBPA^t cluster, but CEBPA bZIP in-frame mutations were almost exclusively present in the CEBPA^t cluster (**Figure 3A,B**).

A comparison of the overall survival between patients in the CEBPA^t cluster showed that all patients in the CEBPA^t cluster had a similarly favourable outcome, irrespective of the CEBPA mutation status (**Figure 3C**). In contrast, patients with a CEBPA mutation outside the CEBPA^t cluster showed inferior overall survival. The CEBPA^t cluster thus marks a favourable AML subtype that extends beyond patients with CEBPA bZIP in-frame mutations and suggests that for subtyping the expression pattern of the CEBPA^t cluster should be considered.

Gene expression profile analysis identifies four transcriptional NPM1 subtypes

Although there have been reports on transcriptional subgroups in NPM1-mutated AML – with clinical implications – the current WHO 2022 and ICC 2022 subclassifications only contain a single NPM1-mutated AML subtype.[2,8,18,19] Based on gene expression profiles, we distinguished four NPM1

clusters with different frequencies of NPM1 mutation-carrying patients in addition to other RGAs (**Figure 4A**), haematological cell types (**Figure 4A-B**), and marker genes (**Figure 4D**).

The NPM1 $(1)^t$ cluster showed enrichment for IDH1-R132, IDH2-R140, and TET2 mutations, with mutual exclusivity between these mutations (**Figure 1D, 4A**). IDH1/2 and TET2 mutations all disrupt TET2-associated pathways[35], indicating that the TET2-pathway disruption drives AML in the NPM1 $(1)^t$ cluster. A similar subset of NPM1-mutated AML with IDH1/2 or TET2 co-mutations, marked by protein expression of CD33 and KIT (CD177) and a lack of CD34 and HLA-DR has been described.[36] NPM1 $(1)^t$ had a corresponding expression pattern for these surface markers, validating this NPM1 subtype (**Supplemental Figure 5**). Besides these earlier reported markers, high gene expression of SNCAIP, PGAM1P5 and SLC22A10 characterised this cluster (**Figure 4D**).

NPM1 $(2)^t$ samples were frequently FLT3-ITD mutated and had a significant higher allele frequency of FLT3-ITD (**Figure 4A,C**). NPM1 and FLT3-ITD mutations thus seem to drive NPM1 $(2)^t$. High expression of GLI2 strongly marked this cluster (**Figure 4D**). The cell-type scores and FAB classification of NPM1$(1)^t$ and NPM1 $(2)^t$ showed a hematopoietic stem cell (HSC) and progenitor-like status, with NPM1 $(1)^t$ samples also displaying high scores for granulocyte-monocyte progenitor (GMP)-like and promonocyte-like expression signatures (**Figure 4A,B**).

NPM1 $(3)^t$ exhibited enrichment for mutations in the FLT3 tyrosine kinase domain (FLT3-TKD), PTPN11, and SMC1A (**Figure 4A**). These mutations generate specific gene expression profiles when co-occurring with an NPM1 mutation.[37–40] NPM1 $(3)^t$ also had a mixed differentiation status pattern while lacking specific marker genes. Therefore, the NPM1 $(3)^t$ cluster seems to be a heterogeneous cluster, consisting of samples with NPM1 mutations and relatively rare co-mutations.

For the NPM1 $(4)^t$ cluster, most samples were co-mutated with DNMT3A-R882 (**Figure 4A**) and had a significantly lower allele frequency for mutated NPM1 (**Figure 4C**). NPM1 $(4)^t$ was characterised mainly by high scores for monocyte-like and conventional dendritic cell (cDC)-like signatures, as reflected by the high fraction of FAB M4 (acute myelomonocytic leukaemia) and M5 (acute monocytic leukaemia) samples (**Figure 4A,B**).

In addition, adult patients from the NPM1 $(1)^t$ and NPM1 $(4)^t$ clusters were older compared to the other NPM1 clusters, while NPM1 $(1)^t$ and NPM1 $(2)^t$ patients were more often female (**Supplemental Figure 6**).

Gene expression profile analysis identifies nine AML-MRC-related transcriptional subtypes

Aside from RGA-defined AML subtypes, the WHO 2022 defines a heterogeneous class of AML-MRC, while the ICC 2022 further divides AML-MRC into three groups based on TP53 mutations, chromatin and splicing gene mutations and cytogenetic abnormalities.[2,8] We found nine AML-MRC-related gene expression-based subtypes, allowing for further stratification of this heterogeneous class.

Only the chromatin and splicing related gene STAG2 marked a cluster, but the other clusters did not encapsulate a single ICC 2022 AML-MRC subtype (**Supplemental Figure 3,4**); AML-MRC $(3)^t$ exemplified this, which showed enrichment for mutations in TP53, RUNX1 and SF3B1 (**Figure 1D, 5A**). AML-MRC subtypes thus mostly do not lead to the specific expression profiles seen for other RGAs, but a further subclassification is possible based on transcriptomics. AML-MRC $(5)^t$ was also enriched for a transcription-induced chimaera between PIM3 and SCO2 that is common in paediatric AML and only detectable by RNA-based methods[41]. The cell-type scores of the AML-MRC-related clusters showed different states of maturational arrest, further indicating that these clusters represent additional subtypes (**Figure 5A,B**).

In addition, we found a novel cluster of IDH1-R132, IDH1-R140, or IDH-R172 mutated samples, indicating that an AML subtype consisting of all IDH1 and IDH2 mutated samples with a specific gene expression should be considered. Tazi and colleagues reported a DNMT3A and IDH1/2 mutated subtype[7], but only half of the IDH1/IDH2 mutations^t cluster patients had a DNMT3A mutation. We found 4% of our patients to be in the IDH1/IDH2 mutations^t cluster, which is four times greater than the incidence reported by Tazi and colleagues.

Finally, we discovered a novel cluster in which we failed to find enrichment for any genetic aberration, which we designated No RGA^t. The No RGA^t cluster showed high expression of genes relating to the T-cells, such as TRAV4 and CD3G (**Figure 5C**).

By further analysis of differential gene expression, we identified marker genes for most AML-MRC clusters – possibly allowing for gene expression-based diagnosis – of which some have also been proposed as therapeutic targets (**Figure 5C**).[42–45] For AML-MRC $(4)^t$, we found high expression of glycophorin genes, which encode transmembrane proteins in red blood cells.[46–48] Indeed, AML-MRC $(4)^t$ had a high proportion of acute erythroid leukaemia AML M6 samples (**Figure 5B**).

Lastly, we inspected the clinical characteristics of the patients in the AML-MRC clusters (**Supplemental Figure 6)**. As expected, AML-MRC patients were older, but we observed this especially

for AML-MRC (6)^t, STAG2^t and No RGA^t. The blast percentages for the AML-MRC clusters varied greatly, with a median blast percentage of 75% for AML-MRC (6)^t and of 30% for AML-MRC (5)^t. The AML-MRC (6)^t cluster had the highest fraction (~50%) of relapsed patients of all 19 clusters.

Novel transcriptional subtypes allow for further risk stratification

Having established new AML subgroups defined by gene expression profiles, we compared differences in overall survival between the clusters to investigate their relevance for risk stratification (**Supplemental Figures 7-8**). Risk stratification for overall survival based on transcriptional subtypes performed equally well compared to genetics.[1,6,7,49] Only the hazard ratio of the KMT2A cluster was higher than expected, which could be attributed to the inclusion of age as a covariable because only younger (<60 years) KMT2A-MLLT3 patients show better survival.[50]

In addition, we investigated if the NPM1 and AML-RMC-related transcriptional clusters provided additional prognostic information. Others have shown differences in survival between NPM1 clusters[19,36], and the NPM1 (2)^t cluster showed a significantly worse outcome based on Cox regression analysis (**Supplemental Figure 9A**). However, no survival differences between the NPM1 clusters remained when we included FLT3-ITD mutation status (**Supplemental Figure 9B**). AML with co-mutation of NPM1 and FLT3-ITD has a known worse outcome than NPM1 mutations alone.[1] The higher hazard ratio of NPM1 (2)^t is thus due to its enrichment for FLT3-ITD mutations, and outcome differences thus seem not haematological maturation stage driven as earlier described.

For the nine AML-MRC clusters we found that AML-MRC (1)^t and AML-MRC (4)^t had relative worse outcomes (**Supplemental Figure 7,8**). Tazi and colleagues[7] observed an intermediate outcome for the DNMT3A-IDH class, but the IDH1/IDH2 mutations^t cluster exhibited a comparable poor outcome to other AML-MRC clusters. In contrast, we found the No RGA^t cluster to be a more favourable AML-MRC subtype (**Supplemental Figure 7,8**) and the AML-MRC-related clusters thus have the potential for risk stratification refinement.

Newly identified AML subtypes exhibit differences in drug response

Finally, we evaluated whether our newly identified gene expression-based AML subtypes are sensitive to specific drugs. Using ex-vivo drug response data, we observed that the NPM1 mutation-enriched clusters exhibited distinct responses to established leukaemia agents such as venetoclax and nilotinib. For the transcriptional AML-MRC clusters, we found cluster-specific drug responses to agents

already used for cancer therapy, possibly improving targeted therapy options for this large AML patient group characterised by a poor prognosis (**Figure 6, Supplemental figure 10**).

For the NPM1^{t} clusters, the Bcl2 protein inhibitor venetoclax – currently in trial for treating AML patients – was effective for NPM1 (1)^{t} and NPM1 (2)^{t}. This result is in line with the finding that monocytic AML phenotype confers resistance to venetoclax, but does not support the finding that FLT3-ITD is associated with increased resistance to venetoclax.[51,52] The ABL inhibitor nilotinib displayed a favourable drug response in NPM1 (3)^{t} and NPM1 (4), similar to the MEK inhibitor selumetinib, which has already shown modest antileukemic activity in patients with AML (**Figure 6A,B, Supplemental Figure 10**).[53] In addition, we also found various drugs to be effective in only one specific NPM1^{t} cluster. For example, the immunomodulatory imide drug lenalidomide was more effective for NPM1 (1)^{t}. The FLT3 inhibitors quizartinib and crenolanib also showed favourable responses for AML in NPM1 (2)^{t}, confirming that this cluster is FLT3-ITD driven (**Figure 6A,B, Supplemental Figure 10**).

For all nine AML-MRC clusters, we found a relatively low resistance to the apoptosis-triggering drug elesclomol but also discovered significant drug response differences between the clusters (**Figure 6A,C, Supplemental Figure 10)**. For example, venetoclax was effective for AML-MRC (2)^{t}, while the CDK9 inhibitor flavopiridol showed more effective killing for AML-MRC(3)^{t} and AML-MRC (5)^{t}.

Finally, we evaluated the drug response of the two novel AML-MRC-related clusters. We could not identify significantly effective drugs for the IDH1/IDH2 mutations^{t} cluster, but the low sample size hindered the analysis of this cluster. In contrast, the No RGA^{t} cluster showed high sensitivity to most drugs and responded particularly well to the second-generation ABL inhibitor dasatinib.

Overall, our data provides new opportunities for targeted therapy in AML, with subtypes based on gene expression rather than recurrent genetic aberrations.

Discussion

Subclassification of AML has made significant progress. However, the subclassification of AML is predominantly genetics-based, while research has shown options for additional stratification using transcriptomics. Therefore, we give in this study an unprecedented overview of transcriptomics in AML, providing a framework for introducing transcriptional subtyping in AML diagnostics.

The scale of this study, due to the integration of several cohorts, permitted extensive analyses and allowed us to identify 19 gene expression-based AML patient groups, many more than are currently in

use based on genetics. We showed vital insights and possibilities for improved subtyping of KMT2A rearranged and CEBPA-mutated AML. In addition, we identify a range of new subtypes in NPM1-mutated AML and AML-MRC, allowing for further stratification of groups that make up 65% of the patients in our dataset. We show the importance of these new patient groups by relating them to specific biological properties, overall survival and ex-vivo drug response profiles, highlighting their potential to benefit AML patients greatly.

Risk stratification guidelines for AML differentiate between KMT2A-MLLT3 and other KMT2A fusions due to different outcomes, which is also reflected in the ICC 2022.[1,8] The prognostic significance of KMT2A rearrangements has been a long topic of debate, with research showing that outcome also depends on expression levels of specific genes and patient age.[50,54] We found that KMT2A-MLLT3, KMT2A-MLLT10 and KMT2A-MLLT1 patients had a similar expression profile, with KMT2A-MLLT4 clustering separately, contrasting the WHO and ICC 2022 subclassifications. We could, however, not evaluate the effects of KMT2A^{t} cluster status on overall survival for individual KMT2A rearrangements due to the availability of outcome data. More data from KMT2A rearranged patients could provide essential insights into the significance of the found KMT2A^{t} cluster and the specific expression profile of KMT2A-MLLT4 for risk stratification.

Similarly, the current genetic CEBPA subtype might be too restrictive since all patients within the CEBPA^{t} cluster had a favourable prognosis. One possible explanation might be the hypermethylation of regulatory CEBPA gene regions, resulting in the same gene expression profile and favourable survival.[55,56] However, the observed incidence of this hypermethylation[56] is too low to explain all cases in the CEBPA^{t} cluster, demonstrating that diagnosis of this favourable subtype should be performed based on gene expression.

We found four transcriptional clusters enriched for AML with mutated NPM1, validating earlier work on NPM1-mutated subgroups with different phenotypes and drug responses[19,36,57] and providing an additional subgroup. However, contrasting earlier work, we found no different survival for the more stem cell-like clusters or NPM1 co-mutated with TET2, IDH1 or IDH2. Only NPM1 (2)^{t} showed a worse outcome, which we could relate to the known worse outcome observed for NPM1 and FLT3-ITD co-mutated patients.[1] Further research will have to investigate the significance of transcriptional NPM1 subtypes for risk assessment. Still, different gene expression-based NPM1 subtypes – with different ex-vivo drug sensitivities – should be considered in updates of AML subclassification guidelines.

For AML-MRC, we found nine subgroups. To our knowledge, we are the first to identify AML-MRC classes with different biological properties, overall survival, and ex-vivo drug responses based on gene expression. Identifying subgroups with specific treatment options for AML-MRC patients is essential since these patients are generally older, have worse clinical outcomes, and often do not qualify for chemotherapy or allogeneic stem cell transplantation.[20,21] Also, no clear targeted therapies besides hypomethylating agents are available for these patients currently[58]. Identifying these nine patient clusters was highly dependent on gene expression – exemplified by the cluster with high T-cell receptor expression – and did not overlap with ICC 2022 definitions, thus underscoring the relevance of transcriptomics in AML diagnostics.

Ideally, the field uses these transcriptional AML subtypes to design new clinical studies to evaluate subtype-specific drug responses. The favourable reaction of AML in two AML-MRC clusters for flavopiridol, a drug for which there are ongoing efforts to identify specific subsets of responsive AML patients, exemplifies the relevance of identifying subtypes with possible specific drug responses.[59] Also, these discoveries can provide a rationale for implementing transcriptomics in AML diagnostics to treat relapsed or refractory AML patients – for whom there are no standard treatment options – with drugs for other cancers.

In conclusion, we show that gene expression analysis of AML identifies various new clinically applicable subtypes of AML, emphasising the relevance of integrating transcriptomics in routine diagnostics. In the future, expression-based AML subclassification could guide personalised treatment decisions, hopefully resulting in improved overall survival and a better quality of life.

Acknowledgements

This project was funded by a strategic investment of the Leiden University Medical Center, embedded within the Leiden Oncology Center, and executed within the Leiden Center for Computational Oncology. EvdA was funded by a personal grant from the Dutch Research Council (NWO; VENI: 09150161810095). The funding bodies had no role in the study design, the collection, analysis, and interpretation of data, the writing of the manuscript, and the decision to submit the manuscript for publication.

Author Contributions

M.J.R., M.G., and E.B.A. conceived and designed the project; E.B.A. acquired funding; E.B.A. performed project administration; M.G., E.B.A., H.V., R.R.B., C.J.M.H., P.B. performed oversight and management of resources (data generation, collection, transfer, infrastructure, data processing); J.F.S. performed computational and statistical analyses; J.F.S., E.B.A., M.G., E.O.K., E.S.-L. performed analyses and interpretation; J.F.S. performed and structured data visualisation; M.J.R., M.G. and E.B.A. provided supervision and scientific direction; J.F.S. wrote the manuscript; and all authors critically reviewed the manuscript and figures.

Disclosure of interest

The authors declare no competing financial interests.

References

1. Döhner H, Wei AH, Appelbaum FR, et al. Diagnosis and management of AML in adults: 2022 recommendations from an international expert panel on behalf of the ELN. *Blood*. 2022;140(12):1345–1377.
2. Khoury JD, Solary E, Abla O, et al. The 5th edition of the World Health Organization Classification of Haematolymphoid Tumours: Myeloid and Histiocytic/Dendritic Neoplasms. *Leukemia*. 2022;36(7):1703–1719.
3. The Cancer Genome Atlas Research Network. Genomic and Epigenomic Landscapes of Adult De Novo Acute Myeloid Leukemia. *N. Engl. J. Med.* 2013;368(22):2059–2074.
4. Farrar JE, Schuback HL, Ries RE, et al. Genomic Profiling of Pediatric Acute Myeloid Leukemia Reveals a Changing Mutational Landscape from Disease Diagnosis to Relapse. *Cancer Res.* 2016;76(8):2197–2205.
5. Tyner JW, Tognon CE, Bottomly D, et al. Functional genomic landscape of acute myeloid leukaemia. *Nat. 2018 5627728*. 2018;562(7728):526–531.
6. Papaemmanuil E, Gerstung M, Bullinger L, et al. Genomic Classification and Prognosis in Acute Myeloid Leukemia. *N. Engl. J. Med.* 2016;374(23):2209–2209.
7. Tazi Y, Arango-Ossa JE, Zhou Y, et al. Unified classification and risk-stratification in Acute Myeloid Leukemia. *Nat. Commun.* 2022;13(1):4622.
8. Arber DA, Orazi A, Hasserjian RP, et al. International Consensus Classification of Myeloid Neoplasms and Acute Leukemias: integrating morphologic, clinical, and genomic data. *Blood*. 2022;140(11):1200–1228.
9. Burd A, Levine RL, Ruppert AS, et al. Precision medicine treatment in acute myeloid leukemia using prospective genomic profiling: feasibility and preliminary efficacy of the Beat AML Master Trial. *Nat. Med.* 2020;26(12):1852–1858.
10. Valk PJM, Verhaak RGW, Beijen MA, et al. Prognostically Useful Gene-Expression Profiles in Acute Myeloid Leukemia. *N. Engl. J. Med.* 2004;350(16):1617–1628.
11. Macrae T, Sargeant T, Lemieux S, et al. RNA-Seq reveals spliceosome and proteasome genes as most consistent transcripts in human cancer cells. *PloS One*. 2013;8(9):e72884.
12. Lavallée V-P, Baccelli I, Krosl J, et al. The transcriptomic landscape and directed chemical interrogation of MLL-rearranged acute myeloid leukemias. *Nat. Genet.* 2015;47(9):1030–1037.
13. Pabst C, Bergeron A, Lavallée V-P, et al. GPR56 identifies primary human acute myeloid leukemia cells with high repopulating potential in vivo. *Blood*. 2016;127(16):2018–2027.
14. Lavallée V-P, Lemieux S, Boucher G, et al. RNA-sequencing analysis of core binding factor AML identifies recurrent ZBTB7A mutations and defines RUNX1-CBFA2T3 fusion signature. *Blood*. 2016;127(20):2498–2501.
15. Mou T, Pawitan Y, Stahl M, et al. The transcriptome-wide landscape of molecular subtype-specific mRNA expression profiles in acute myeloid leukemia. *Am. J. Hematol.* 2021;96(5):580–588.

16. Wouters BJ, Löwenberg B, Erpelinck-Verschueren CAJ, et al. Double CEBPA mutations, but not single CEBPA mutations, define a subgroup of acute myeloid leukemia with a distinctive gene expression profile that is uniquely associated with a favorable outcome. *Blood*. 2009;113(13):3088–3091.
17. Taskesen E, Bullinger L, Corbacioglu A, et al. Prognostic impact, concurrent genetic mutations, and gene expression features of AML with CEBPA mutations in a cohort of 1182 cytogenetically normal AML patients: further evidence for CEBPA double mutant AML as a distinctive disease entity. *Blood*. 2011;117(8):2469–2475.
18. Verhaak RGW, Goudswaard CS, Van Putten W, et al. Mutations in nucleophosmin (NPM1) in acute myeloid leukemia (AML): association with other gene abnormalities and previously established gene expression signatures and their favorable prognostic significance. *Blood*. 2005;106(12):3747–3754.
19. Mer AS, Heath EM, Madani Tonekaboni SA, et al. Biological and therapeutic implications of a unique subtype of NPM1 mutated AML. *Nat. Commun.* 2021;12(1):1054.
20. de Leeuw DC, Ossenkoppele GJ, Janssen JJWM. Older Patients with Acute Myeloid Leukemia Deserve Individualized Treatment. *Curr. Oncol. Rep.* 2022;24(11):1387–1400.
21. Improved relative survival in older patients with acute myeloid leukemia over a 30-year period in the Netherlands: a long haul is needed to change nothing into something | Leukemia.
22. Arindrarto W, Borràs DM, de Groen RAL, et al. Comprehensive diagnostics of acute myeloid leukemia by whole transcriptome RNA sequencing. *Leuk. 2020 351*. 2020;35(1):47–61.
23. Putri GH, Anders S, Pyl PT, Pimanda JE, Zanini F. Analysing high-throughput sequencing data in Python with HTSeq 2.0. *Bioinformatics*. 2022;38(10):2943–2945.
24. Frankish A, Diekhans M, Jungreis I, et al. GENCODE 2021. *Nucleic Acids Res.* 2021;49(D1):D916–D923.
25. Zhang Y, Parmigiani G, Johnson WE. ComBat-seq: batch effect adjustment for RNA-seq count data. *NAR Genomics Bioinforma.* 2020;2(3):lqaa078.
26. Büttner M, Miao Z, Wolf FA, Teichmann SA, Theis FJ. A test metric for assessing single-cell RNA-seq batch correction. *Nat. Methods*. 2019;16(1):43–49.
27. Love MI, Huber W, Anders S. Moderated estimation of fold change and dispersion for RNA-seq data with DESeq2. *Genome Biol.* 2014;15(12):550.
28. Traag VA, Waltman L, van Eck NJ. From Louvain to Leiden: guaranteeing well-connected communities. *Sci. Rep.* 2019;9(1):5233.
29. van Galen P, Hovestadt V, Wadsworth II MH, et al. Single-Cell RNA-Seq Reveals AML Hierarchies Relevant to Disease Progression and Immunity. *Cell*. 2019;176(6):1265-1281.e24.
30. Nagel S, Pommerenke C, Meyer C, MacLeod RAF, Drexler HG. Aberrant expression of NKL homeobox genes HMX2 and HMX3 interferes with cell differentiation in acute myeloid leukemia. *PLOS ONE*. 2020;15(10):e0240120.
31. Nakagawa K, Noguchi Y, Uenaka A, et al. XAGE-1 expression in non-small cell lung cancer and antibody response in patients. *Clin. Cancer Res. Off. J. Am. Assoc. Cancer Res.* 2005;11(15):5496–5503.
32. Yazdi MT, Loof NM, Annema JT, et al. XAGE-1b and p53: Potential targets for immunotherapy of non-small cell lung cancer (NSCLC). *Eur. Respir. J.* 2012;40(Suppl 56):
33. Wakita S, Sakaguchi M, Oh I, et al. Prognostic impact of CEBPA bZIP domain mutation in acute myeloid leukemia. *Blood Adv.* 2022;6(1):238–247.
34. Taube F, Georgi JA, Kramer M, et al. CEBPA mutations in 4708 patients with acute myeloid leukemia: differential impact of bZIP and TAD mutations on outcome. *Blood*. 2022;139(1):87–103.
35. Inoue S, Lemonnier F, Mak TW. Roles of IDH1/2 and TET2 mutations in myeloid disorders. *Int. J. Hematol.* 2016;103(6):627–633.
36. Mason EF, Kuo FC, Hasserjian RP, Seegmiller AC, Pozdnyakova O. A distinct immunophenotype identifies a subset of NPM1-mutated AML with TET2 or IDH1/2 mutations and improved outcome. *Am. J. Hematol.* 2018;93(4):504–510.
37. Fobare S, Kohlschmidt J, Ozer HG, et al. Molecular, clinical, and prognostic implications of PTPN11 mutations in acute myeloid leukemia. *Blood Adv.* 2022;6(5):1371–1380.
38. Eisfeld A-K, Kohlschmidt J, Mims A, et al. Additional gene mutations may refine the 2017 European LeukemiaNet classification in adult patients with de novo acute myeloid leukemia aged <60 years. *Leukemia*. 2020;34(12):3215–3227.
39. Simonetti G, Mengucci C, Padella A, et al. Integrated genomic-metabolic classification of acute myeloid leukemia defines a subgroup with NPM1 and cohesin/DNA damage mutations. *Leukemia*. 2021;35(10):2813–2826.
40. Boddu P, Kantarjian H, Borthakur G, et al. Co-occurrence of FLT3-TKD and NPM1 mutations

defines a highly favorable prognostic AML group. *Blood Adv.* 2017;1(19):1546–1550.
41. Kuhn J, Meerzaman D, Ries RE, et al. PIM3-SCO2 Fusion Is a Novel Transcription-Induced Chimera That Is Highly Prevalent In Childhood AML. *Blood*. 2013;122(21):2549.
42. Sazinsky S, Nguyen P, Zafari M, et al. 886 Targeting VSIG4, a novel macrophage checkpoint, repolarizes suppressive macrophages which induces an inflammatory response in primary cell in vitro assays and fresh human tumor cultures. *J. Immunother. Cancer*. 2021;9(Suppl 2):
43. Liu W, Yu C, Li J, Fang J. The Roles of EphB2 in Cancer. *Front. Cell Dev. Biol.* 2022;10:.
44. Allain EP, Rouleau M, Lévesque E, Guillemette C. Emerging roles for UDP-glucuronosyltransferases in drug resistance and cancer progression. *Br. J. Cancer*. 2020;122(9):1277–1287.
45. Banús-Mulet A, Etxabe A, Cornet-Masana JM, et al. Serotonin receptor type 1B constitutes a therapeutic target for MDS and CMML. *Sci. Rep.* 2018;8:13883.
46. Hollox EJ, Louzada S. Genetic variation of glycophorins and infectious disease. *Immunogenetics*. 2022;
47. Greaves MF, Sieff C, Edwards PAW. Monoclonal Antiglycophorin as a Probe for Erythroleukemias. *Blood*. 1983;61(4):645–651.
48. Andersson LC, Gahmberg CG, Teerenhovi L, Vuopio P. Glycophorin a as a cell surface marker of early erythroid differentiation in acute leukemia. *Int. J. Cancer*. 1979;24(6):717–720.
49. Shiba N, Ichikawa H, Taki T, et al. NUP98-NSD1 gene fusion and its related gene expression signature are strongly associated with a poor prognosis in pediatric acute myeloid leukemia. *Genes. Chromosomes Cancer*. 2013;52(7):683–693.
50. Bill M, Mrózek K, Kohlschmidt J, et al. Mutational landscape and clinical outcome of patients with de novo acute myeloid leukemia and rearrangements involving 11q23/*KMT2A*. *Proc. Natl. Acad. Sci.* 2020;117(42):26340–26346.
51. Pei S, Pollyea DA, Gustafson A, et al. Monocytic Subclones Confer Resistance to Venetoclax-Based Therapy in Acute Myeloid Leukemia Patients. *Cancer Discov.* 2020;10(4):536–551.
52. Griffioen MS, de Leeuw DC, Janssen JJWM, Smit L. Targeting Acute Myeloid Leukemia with Venetoclax; Biomarkers for Sensitivity and Rationale for Venetoclax-Based Combination Therapies. *Cancers*. 2022;14(14):3456.
53. Jain N, Curran E, Iyengar NM, et al. Phase II study of the oral MEK inhibitor selumetinib in advanced acute myelogenous leukemia: a University of Chicago phase II consortium trial. *Clin. Cancer Res. Off. J. Am. Assoc. Cancer Res.* 2014;20(2):490–498.
54. Noordermeer SM, Sanders MA, Gilissen C, et al. High BRE expression predicts favorable outcome in adult acute myeloid leukemia, in particular among MLL-AF9–positive patients. *Blood*. 2011;118(20):5613–5621.
55. Lin T-C, Hou H-A, Chou W-C, et al. CEBPA methylation as a prognostic biomarker in patients with de novo acute myeloid leukemia. *Leukemia*. 2011;25(1):32–40.
56. Hollink IHIM, van den Heuvel-Eibrink MM, Arentsen-Peters STCJM, et al. Characterization of CEBPA mutations and promoter hypermethylation in pediatric acute myeloid leukemia. *Haematologica*. 2011;96(3):384–392.
57. Cheng W-Y, Li J-F, Zhu Y-M, et al. Transcriptome-based molecular subtypes and differentiation hierarchies improve the classification framework of acute myeloid leukemia. *Proc. Natl. Acad. Sci.* 2022;119(49):e2211429119.
58. DiNardo CD, Jonas BA, Pullarkat V, et al. Azacitidine and Venetoclax in Previously Untreated Acute Myeloid Leukemia. *N. Engl. J. Med.* 2020;383(7):617–629.
59. Boffo S, Damato A, Alfano L, Giordano A. CDK9 inhibitors in acute myeloid leukemia. *J. Exp. Clin. Cancer Res.* 2018;37(1):36.

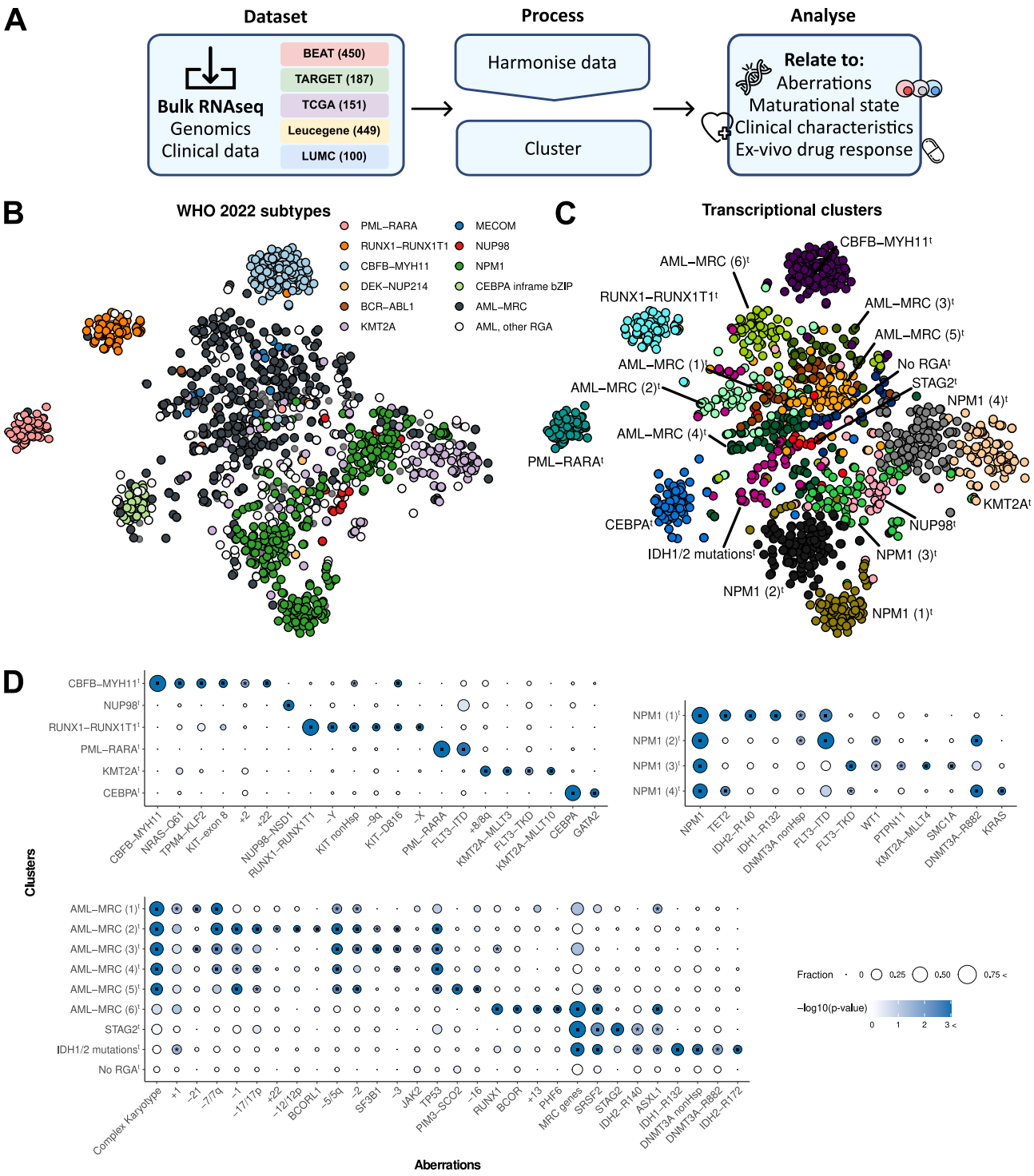

Figure 1: Transcriptomic analysis further stratifies AML. A) Flowchart of the used methods. **B)** A tSNE of the expression of the 2000 most variable genes per the median absolute deviation (MAD). Each dot represents a patient sample. The samples are coloured according to the WHO 2022 subtyping of AML. **C)** The same tSNE as in **B**, but samples are coloured according to one of the 19 clusters found using the Leiden algorithm. Cluster names are based on enriched aberrations. **D)** Dot plots that show aberration enrichment in the 19 found clusters, using Fisher's extract test. The dots are coloured according to the corrected p-value. The p-values were corrected for multiple testing using the Benjamini-Hochberg procedure. The dots are sized according to the fraction of samples in the cluster with the aberration. The x-axis shows the aberrations and the y-axis shows the clusters.

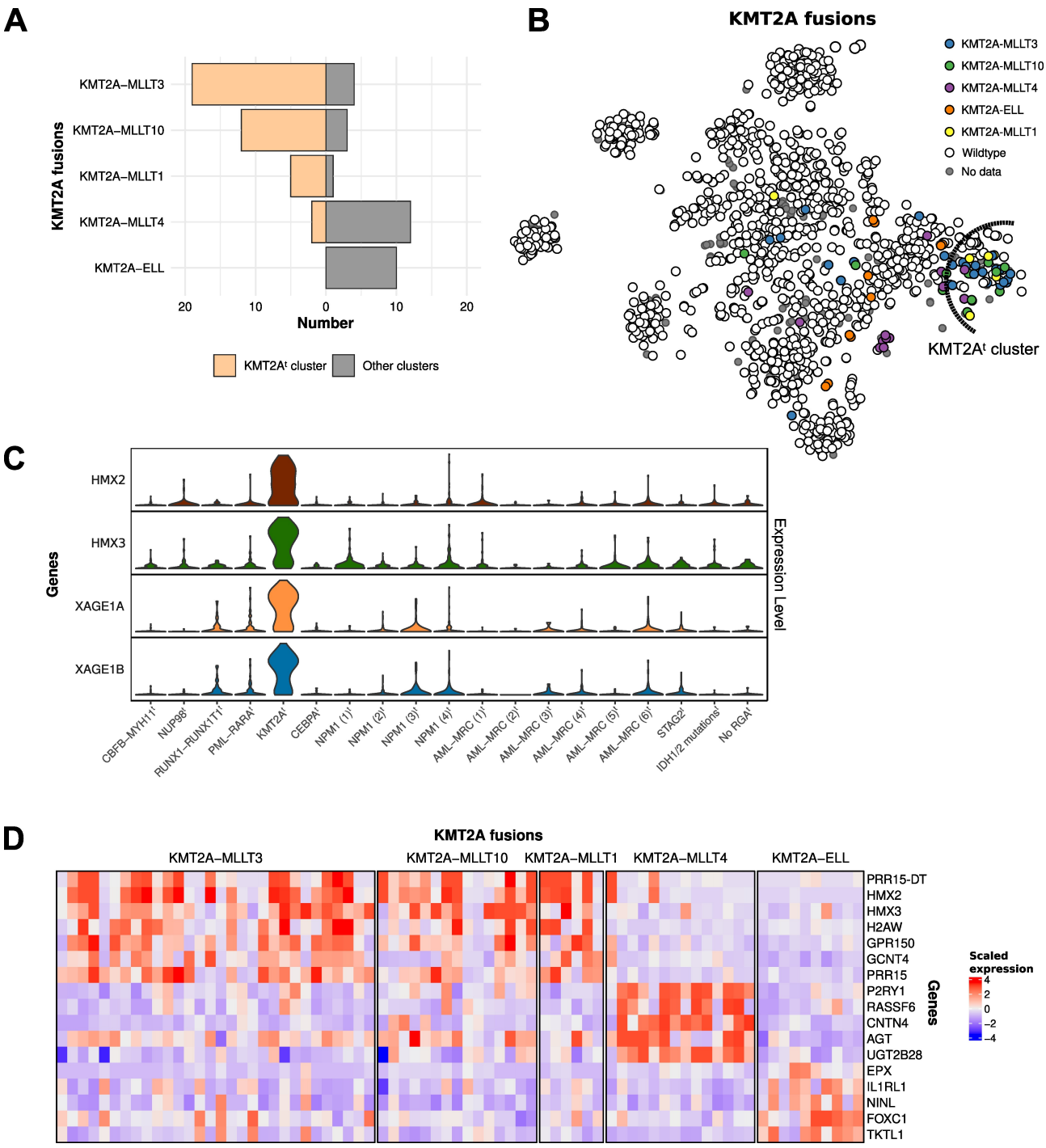

Figure 2: KMT2A fusions with MLLT3, MLLT10, and MLLT1 share a specific gene expression signature. A) shows the number of KMT2A arrangements with different fusion partners found in the KMT2Aᵗ cluster and the combined other clusters. Only KMT2A fusions with five or more cases are shown. **B)** tSNE based on the 2000 most variable genes. The samples are coloured according to KMT2A-fusions in A. **C)** Violin plots of the expression of marker genes for the KMT2Aᵗ cluster. **D)** Heatmap showing the differential expression of marker genes for the fusions in **A**. The columns are samples, which are split according to fusions. The rows are the genes.

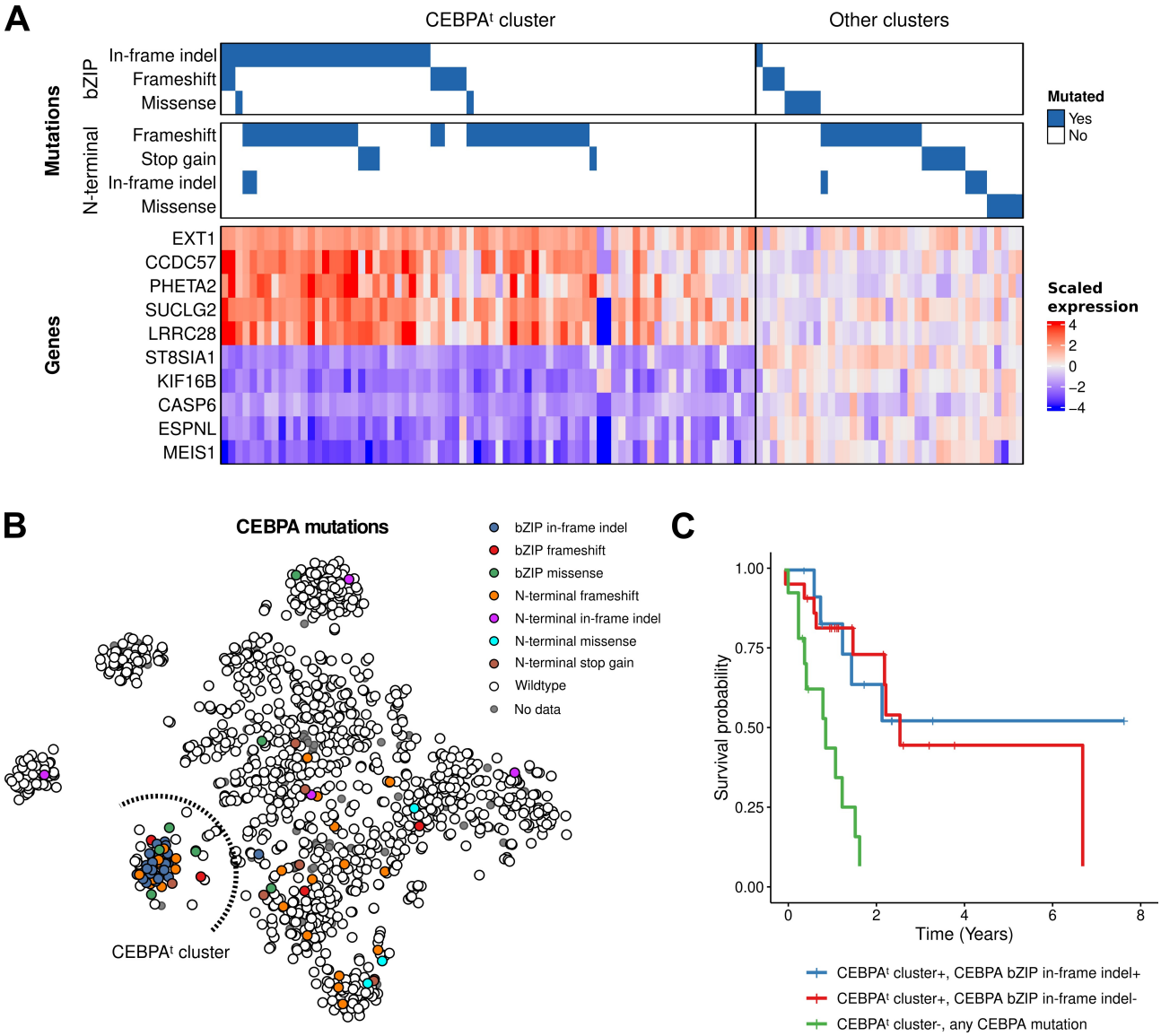

Figure 3: The CEBPA^t cluster gene expression signature indicates a favourable prognosis even in absence of a CEBPA bZIP in-frame mutation. A) Waterfall plot and gene expression heatmap of all samples in the CEBPA^t cluster and samples with a CEBPA mutation located outside the CEBPA^t cluster. For the waterfall plot, the rows are the type and location of the mutation in the CEBPA gene. The heatmap shows the expression of marker genes for the CEBPA^t cluster, with the specific genes on the rows. The columns are the samples, grouped by CEPBA^t cluster or the combined other clusters. **B)** tSNE based on the 2000 most variable genes. The samples are coloured according to the type of CEBPA mutation. **C)** Kaplan-Meier curve of the survival of samples in and outside the CEBPA^t cluster. In blue is the survival curve of patients in the CEBPA^t cluster with a CEBPA bZIP in-frame indel. In red are the patients in the CEBPA^t cluster without a CEBPA bZIP in-frame mutaions. In green are the patients with a CEBPA mutation located outside of the CEBPA^t cluster.

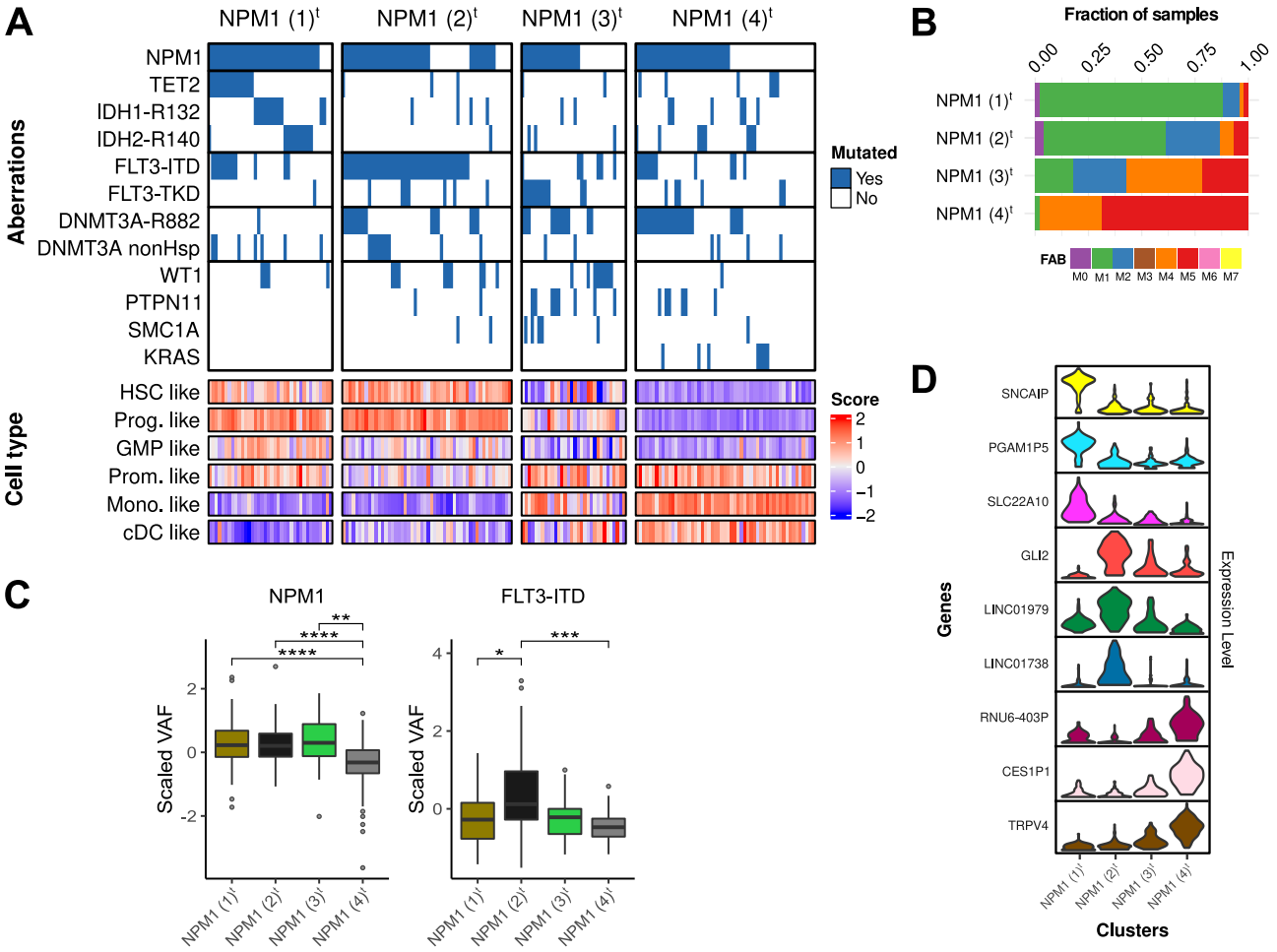

Figure 4: Gene expression profile analysis identifies four transcriptional NPM1 subtypes. A) Waterfall plot of enriched mutations in the NPM1 clusters, combined with a plot of the cell type scores for different haematological cells. The cell type score was generated by taking the mean expression of 30 marker genes per cell type. The columns are samples grouped by cluster. The rows are the aberrations and cell type scores. Only samples with data on all enriched aberrations are plotted. **B)** Barplot showing the fraction of different FAB classifications found in the four NPM1 clusters. **C)** Boxplots showing the scaled variant allele frequency (VAF) of mutated NPM1 and FLT3-ITD from the BEAT, Leucegene, and LUMC cohorts. The VAF was scaled per gene and study to allow for a combined analysis. We used a Wilcoxon test to test for significant differences in VAFs between the clusters. The Benjamini-Hochberg procedure was used to adjust the p-values for multiple testing. P-values: * < 0.05, ** < 0.01, *** < 0.001 **D)** Violin plots of the expression of marker genes for the NPM1-enriched clusters. HSC = hematopoietic stem cells, Prog. = progenitor, GMP = granulocyte-monocyte progenitor, Prom. = promonocytes, Mono. = monocytes, cDC = conventional dendritic cells, FAB = French American British classification, VAF = variant allele frequency

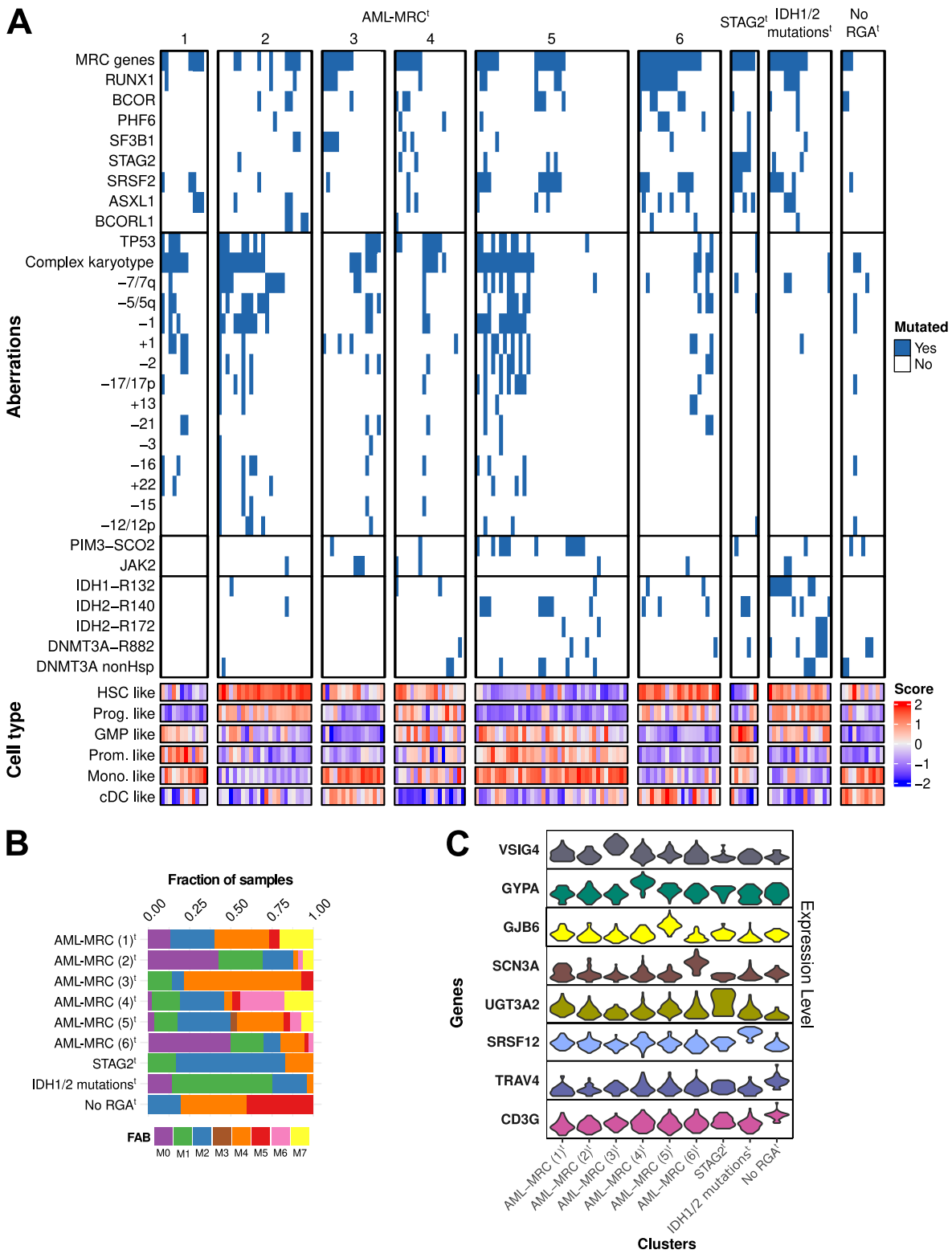

Figure 5: Gene expression profile analysis identifies nine AML-MRC-related transcriptional subtypes. A) Waterfall plot of the enriched mutations in the nine AML-MRC-related clusters, combined with a plot of cell type scores for various haematological cells. We generated cell type scores by taking the mean of 30 marker genes per cell type. The columns are samples, split per cluster. The rows are the aberrations and scores. Only samples with data on all enriched aberrations are plotted. MRC genes signifies a mutation in ASXL1, BCOR, EZH2, RUNX1, SF3B1, SRSF2, STAG2, U2AF1, or ZRSR2. **B)** Barplot showing the fraction of different FAB classifications found in the nine AML-MRC-related clusters. **C)** Violin plots of the expression of marker genes for the nine novel AML-MRC clusters, HSC = hematopoietic stem cells, Prog. = progenitor, GMP = granulocyte-monocyte progenitor, Prom. = promonocytes, Mono. = monocytes, cDC = conventional dendritic cells, FAB = French American British classification, AML-MRC = Acute myeloid leukemia with myelodysplasia-related changes

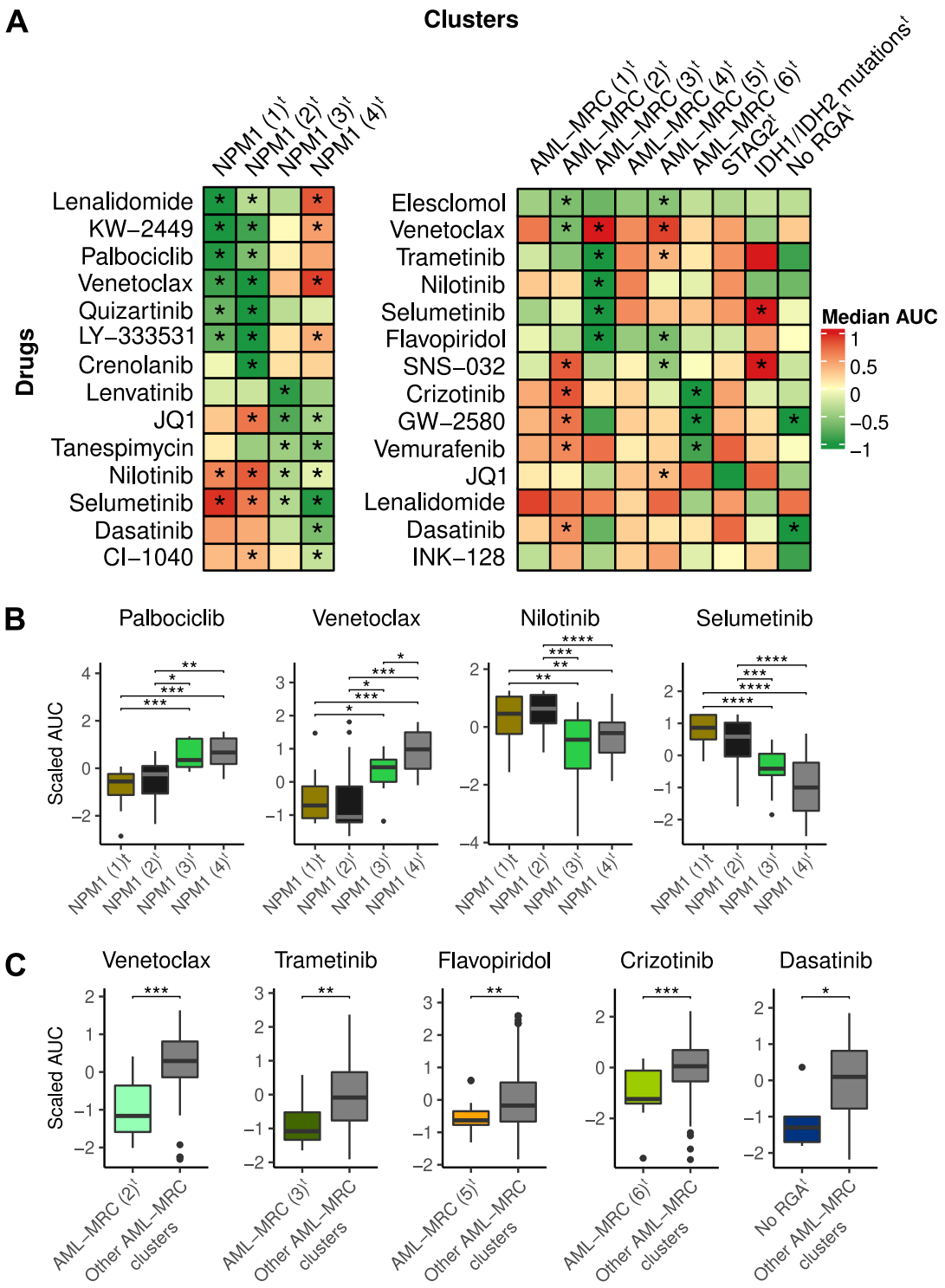

Figure 6: Newly identified AML subtypes exhibit differences in drug response. A) Heatmap plots coloured according to the median scaled area under the curve (AUC) of the ex-vivo drug response per drug and cluster. A green colour indicates a lower median AUC for the drug for the samples in the cluster compared to the other clusters, which means that a lower dosage was required to kill the same amount of cells and thus indicating a better drug response. Red indicates a higher median AUC, meaning an unfavourable drug response. An asterisk indicates a significant lower or higher AUC compared to the combined other clusters (p-value < 0.05) according to a Wilcoxon test. We corrected the resulting p-values with the Benjamini-Hochberg (BH) procedure. The heatmaps show a selection of results from Supplemental Figure 10. **B)** Boxplots showing ex-vivo drug response per NPM1 cluster. **C)** Same as **B**, but for the AML-MRC clusters. For **B** and **C**, we performed significance testing using the Wilcoxon test, and p-values were corrected using the BH procedure. P-values for boxplots: * < 0.05, ** < 0.01, *** < 0.001, **** < 0.0001.